Available online at www.sciencedirect.com

SCIENCE DIRECT

Journal of Sound and Vibration 297 (2006) 183–199

JOURNAL OF SOUND AND VIBRATION

www.elsevier.com/locate/jsvi

Nonresonant Hopf bifurcations of a controlled van der Pol–Duffing oscillator

J.C. Ji*

School of Mechanical Engineering, The University of Adelaide, SA 5005, Australia

Received 15 August 2005; received in revised form 7 March 2006; accepted 17 March 2006
Available online 9 June 2006

Abstract

The trivial equilibrium of a van der Pol–Duffing oscillator with a nonlinear feedback control may lose its stability via Hopf bifurcations, when the time delay involved in the feedback control reaches certain values. Nonresonant Hopf–Hopf interactions may occur in the controlled van der Pol–Duffing oscillator when the corresponding characteristic equation has two pairs of purely imaginary roots. With the aid of normal form theory and centre manifold theorem as well as a perturbation method, the dynamic behaviour of the nonresonant co-dimension two bifurcation is investigated by studying the possible solutions and their stability of the four-dimensional ordinary differential equations on the centre manifold. In the vicinity of the nonresonant Hopf bifurcation, the oscillator may exhibit the initial equilibrium solution, two periodic solutions as well as a quasi-periodic solution on a two-dimensional torus, depending on the dummy unfolding parameters and nonlinear terms. The analytical predictions are found to be in good agreement with the results of numerical integration of the original delay differential equation.

1. Introduction

The well-known van der Pol–Duffing oscillator has been shown to exhibit very rich dynamics including chaotic, quasi-periodic and periodic behaviour [1–6]. Chaotic and quasi-periodic motions as well as large amplitude vibrations may be undesirable and unwanted in many applications for the control of oscillations. Much effort has been devoted to controlling the dynamics of van der Pol–Duffing oscillators, using a nonlinear feedback control [7–9] or a delayed feedback control [10–14]. However, either unavoidable time delays in the feedback path or deliberately implemented time delays in the controllers and actuators may lead to complicated dynamics and induce instability of the controlled systems. Thus, a detailed study of the effect of time delays on the dynamics of the controlled systems is a desirable task for the evaluation of the control performance. The present paper is mainly focused on the underlying dynamics of a controlled van der Pol–Duffing oscillator that follows a nonresonant co-dimension two bifurcation of Hopf–Hopf interactions.

*Tel.: +61 8 8303 6941; fax: +61 8 8303 4367.
E-mail address: jcji@mecheng.adelaide.edu.au.

0022-460X/$ - see front matter
doi:10.1016/j.jsv.2006.03.043

An externally forced van der Pol–Duffing oscillator under a feedback control considered in the present paper is of the form

$$\ddot{x} - (\mu - \beta x^2)\dot{x} + \omega^2 x + \alpha x^3 = e\cos(\Omega_0 t) + f_c(t), \tag{1}$$

where x is the displacement, ω is the natural frequency, α is the coefficient of the nonlinear term, $\mu > 0$, $\beta > 0$, e and Ω_0 represent the amplitude and frequency of the external excitation, respectively, $f_c(t)$ is the feedback control input, and an overdot indicates the differentiation with respect to time t. Without loss of generality, it is assumed that the feedback control used is of a linear-plus-nonlinear characteristic, which takes the form of

$$f_c(t) = px(t-\tau) + q\dot{x}(t-\tau) + k_1 x^3(t-\tau) + k_2\dot{x}^3(t-\tau) + k_3\dot{x}(t-\tau)x^2(t-\tau) + k_4\dot{x}^2(t-\tau)x(t-\tau), \tag{2}$$

where p and q are the proportional and derivative linear feedback gains, k_i are the weakly nonlinear feedback gains, and τ denotes the time delay occurring in the feedback path. Only one time delay is considered here for the sake of simplicity.

It was found that the trivial equilibrium of the corresponding autonomous system of Eq. (1) may change its stability via a Hopf bifurcation if the time delay reaches certain values. When the corresponding characteristic equation has two pairs of purely imaginary roots, it was shown that the trivial equilibrium of the autonomous system may lose its stability via a subcritical or supercritical Hopf bifurcation and regain its stability via a reverse subcritical or supercritical Hopf bifurcation as the time delay increases. There are a number of switches between stability and instability of the trivial equilibrium, and the trivial equilibrium eventually becomes unstable. A stable limit cycle appears after a supercritical Hopf bifurcation occurs and disappears through a reverse supercritical Hopf bifurcation [15].

It is expected that an interaction of two Hopf bifurcations may occur when the two corresponding critical time delays have the same value. The points of intersection of two Hopf bifurcations usually occur on the boundary of the region of stability of the trivial equilibrium. Hence, intersections of Hopf bifurcations may influence the observed behaviour of the system. Complicated behaviour may be expected to appear in the neighbourhood of the intersection point. The primary objective of the present paper is to study the dynamics of the controlled system in the vicinity of the point of intersection of nonresonant Hopf–Hopf bifurcations. The present paper develops the existing relevant work in at least the following three aspects: (a) the variations of the controller's parameters (which are two linear feedback gains and time delay) in the vicinity of the nonresonant co-dimension two bifurcation are introduced by three dummy perturbation parameters. These perturbation parameters eventually determine the unfolding parameters of the normal forms of Hopf–Hopf interactions. However, the unfolding parameters given in the published work were artificially added to the normal forms of the degenerate system [16]. (b) The present paper gives a detailed analysis of the bifurcations and possible solutions of the system in the neighbourhood of nonresonant Hopf bifurcations, while existing works gave limited numerical results only [17]. (c) Illustrative examples are given to validate the analytical predictions of the bifurcation solutions.

The present paper is organized into six parts. The existence of a double Hopf bifurcation is briefly reviewed in Section 2 for the corresponding autonomous system. In Section 3, based on semigroups of transformations and the decomposition theory, the delay differential equation in the neighbourhood of nonresonant Hopf bifurcations is reduced to a set of four-dimensional (4D) nonlinear ordinary differential equations on the centre manifold. The steady-state solutions of these ordinary differential equations are studied in Section 4 using a perturbation method. In Section 5, examples are given to illustrate the observed behaviour of a specific system in the neighbourhood of the nonresonant co-dimension two bifurcation. The summary and discussion are presented in Section 6.

2. Double Hopf bifurcation

The analysis is started from the corresponding autonomous system for which the external excitation is neglected in Eq. (1), as an understanding of the dynamics of the autonomous system lays the foundation of exploring the rich dynamic behaviour of the system with external forcing. The stability of the trivial equilibrium and the resultant behaviour of the autonomous system that follows a nonresonant Hopf bifurcation will be investigated using the centre manifold theorem and normal form theory as well as the method of multiple scales. The forced response of the non-autonomous system (1) in the vicinity of nonresonant Hopf bifurcations is beyond the scope of the present work, but should be pursued further. The corresponding autonomous system, obtained by letting $e = 0$ in Eq. (1), is given by

$$\ddot{x} - \mu\dot{x} + \omega^2 x - px(t-\tau) - q\dot{x}(t-\tau) + \beta x^2\dot{x} + \alpha x^3 - k_1x^3(t-\tau) - k_2\dot{x}^3(t-\tau) \\ - k_3\dot{x}(t-\tau)x^2(t-\tau) - k_4\dot{x}^2(t-\tau)x(t-\tau) = 0. \tag{3}$$

It is easy to note that Eq. (3) has either one or three fixed points depending on the system parameters. If $(\omega^2 - p)/(k_1 - \alpha) > 0$, there are three fixed points, which are the trivial point, and two non-trivial fixed points at $\pm\sqrt{(\omega^2 - p)/(k_1 - \alpha)}$. Otherwise, Eq. (3) has the trivial fixed point only. A discussion of the stability of the trivial fixed point appears to be of interest. In fact, the stability characteristic of the non-trivial fixed points can be investigated in a similar procedure by converting them into the trivial fixed point using a linear coordinate transformation. To study the local stability of the trivial fixed point, it is usual to seek a candidate solution of the form $c\exp(\lambda t)$, where c is a constant. Substitution of the candidate solution in the linearized part of Eq. (3) leads to the following characteristic equation

$$\lambda^2 - \mu\lambda + \omega^2 - p\mathrm{e}^{-\lambda\tau} - q\lambda\mathrm{e}^{-\lambda\tau} = 0. \tag{4}$$

The roots of the characteristic Eq. (4) are a function of the time delay, τ. If there is no time delay involved in the system, i.e., $\tau = 0$, ensuring the stability of the trivial fixed point requires that $q < -\mu$ and $p < \omega^2$. It will be shown that these two inequalities cannot guarantee the stability of the trivial point of the controlled system involving time delay. By the continuity of the solutions of Eq. (4), as the time delay increases, the purely imaginary roots of Eq. (4) may appear while all the other eigenvalues have negative real parts. It is assumed that a pair of purely imaginary eigenvalues of Eq. (4) occurs at $\lambda = \pm\mathrm{i}\delta$, where $\mathrm{i} = \sqrt{-1}$, and δ is a real positive number. Substituting $\lambda = \mathrm{i}\delta$ in Eq. (4) and separating the real and imaginary parts yields

$$\omega^2 - \delta^2 - p\cos(\delta\tau) - \delta q\sin(\delta\tau) = 0, \\ -\mu\delta + p\sin(\delta\tau) - q\delta\cos(\delta\tau) = 0. \tag{5}$$

Moving the trigonometric terms to the right-hand side of Eq. (5), squaring both sides of the resultant equations and adding them together yields

$$(\omega^2 - \delta^2)^2 + \mu^2\delta^2 = p^2 + q^2\delta^2. \tag{6}$$

Its roots are

$$\delta_\pm^2 = \frac{1}{2}\left(q^2 - \mu^2 + 2\omega^2 \pm \sqrt{4(p^2 - \omega^4) + (2\omega^2 + q^2 - \mu^2)^2}\right). \tag{7}$$

It is easy to note that δ may have one or two positive solutions depending on the system parameters. If $p^2 \geqslant \omega^4$, Eq. (4) has one pair of purely imaginary solutions only, which is given by $\lambda = \pm\mathrm{i}\delta_+$, with $\delta_+ > 0$. The trivial point of the system may lose its stability via a Hopf bifurcation. The direction and stability of the Hopf bifurcation have been studied for single-degree-of-freedom nonlinear systems involving time delays [15,18–20]. As such this case is not discussed in the present paper.

If $(q^2 - \mu^2 + 2\omega^2) > 0$, and $(\mu^2 - q^2)((1/4)q^2 - (1/4)\mu^2 + \omega^2) < p^2 < \omega^4$, Eq. (4) has two pairs of purely imaginary solutions, which are given by $\lambda_\pm = \pm\mathrm{i}\delta_\pm$, with $\delta_+ > \delta_- > 0$. Such a case is referred to here as a double Hopf bifurcation, which can be regarded as a combination of two single Hopf bifurcations occurring consecutively with an increase of time delay.

Two sets of the critical time delay τ_c corresponding to the two pairs of purely imaginary eigenvalues are given by

$$\tau_{1c,n} = \frac{s_1}{\delta_+} + \frac{2n\pi}{\delta_+}, \quad n = 0, 1, 2\ldots, \tag{8a}$$

where $0 \leqslant s_1 < 2\pi$, $\sin s_1 = (\mu p + q\omega^2 - q\delta_+^2)\delta_+/p^2 + q^2\delta_+^2$, $\cos s_1 = p\omega^2 - p\delta_+^2 - \mu q\delta_+^2/p^2 + q^2\delta_+^2$;

and

$$\tau_{2c,n} = \frac{s_2}{\delta_-} + \frac{2n\pi}{\delta_-}, \tag{8b}$$

where $0 \leqslant s_2 < 2\pi$, $\sin s_2 = (\mu p + q\omega^2 - q\delta_-^2)\delta_-/p^2 + q^2\delta_-^2$, $\cos s_2 = p\omega^2 - p\delta_-^2 - \mu q\delta_-^2/p^2 + q^2\delta_-^2$.

The transversality condition for assuring the occurrence of a double Hopf bifurcation can be easily checked by studying $(\mathrm{d}\tau/\mathrm{d}\lambda)$ instead of $(\mathrm{d}\lambda/\mathrm{d}\tau)$. It is found by performing some algebraic manipulation that the real part of $(\mathrm{d}\tau/\mathrm{d}\lambda)$ at $\lambda = \mathrm{i}\delta$, namely $\mathrm{Re}(\mathrm{d}\tau/\mathrm{d}\lambda)|_{\lambda=\mathrm{i}\delta}$, is given by

$$\mathrm{Re}(\mathrm{d}\tau/\mathrm{d}\lambda)|_{\lambda=\mathrm{i}\delta} = \frac{-q^2}{p^2 + q^2\delta^2} + \frac{\mu^2 + 2\delta^2 - 2\omega^2}{\mu^2\delta^2 + (\omega^2 - \delta^2)^2}. \tag{9}$$

By inserting the expressions of $\delta_\pm^2$, it is easy to find that the quantity $\mathrm{Re}(\mathrm{d}\tau/\mathrm{d}\lambda)|_{\lambda=\mathrm{i}\delta}$ is positive for δ_+^2 and negative for δ_-^2, thereby confirming the transversality conditions for the occurrence of a double Hopf bifurcation [21]. The crossing of the imaginary axis is from left to right as τ increases to a certain value corresponding to δ_+, and crossing from right to left occurs for the certain values of τ corresponding to δ_-. For clarity, the bifurcations occurring at points $(\delta_+, \tau_{1c,n})$ and $(\delta_-, \tau_{2c,n})$ will be termed the first and second single Hopf bifurcations, respectively. The frequencies of the first and second Hopf bifurcations, namely δ_{01} and δ_{02}, are then given by $\delta_{01} = \delta_+$, $\delta_{02} = \delta_-$.

For a double Hopf bifurcation, it follows that $\tau_{1c,0} < \tau_{2c,0}$, since the multiplicities of the roots with positive real parts of Eq. (4) can change only if a root appears on or crosses the imaginary axis as time delay τ varies. As τ increases, the zero solution loses its stability whenever τ passes through a certain value of $\tau_{1c,n}$ and the zero solution regains its stability whenever τ passes through a value of $\tau_{2c,n}$. There are a finite number of switches between the stability and instability of the zero solution, and the zero solution eventually become unstable.

When Eq. (4) has two pairs of purely imaginary eigenvalues, an intersection of the first and second Hopf bifurcations may occur before the zero solution eventually becomes unstable. Points of intersection may be given based on the fact that the two critical time delays related to two Hopf bifurcation frequencies δ_{01} and δ_{02} are identical. Such intersections generally occur in two cases, either nonresonant or resonant Hopf–Hopf interactions, depending on the ratio of the two Hopf bifurcation frequencies. Resonant Hopf bifurcations may occur when the two frequencies of Hopf bifurcations obey $\delta_{01} : \delta_{02} = m : n$ for some $m, n \in Z$. The possible points of the intersection of nonresonant and resonant Hopf bifurcations cannot be given in a closed form, except when there are certain restrictions on the parameter values. The restrictions generally lead to simplified systems, for example, as the case discussed in Ref. [22], in which the damping and a feedback gain were set to be zero. Owing to a nonzero damping and two linear feedback gains involved in Eq. (3), more complicated expressions have been derived for the critical time delays given by Eq. (8). For a given set of the system parameters, the points of intersection of nonresonant and resonant Hopf bifurcations can be solved by a numerical procedure only for the controlled system considered in the present paper.

As an illustrative example, consider a specific system with the parameters given by $\mu = 0.1$, $\omega = 1.0$, $p = -0.4$, $\alpha = 0.4$, $\beta = 0.5$, $k_1 = 0.2$, $k_4 = 0.5$, $k_2 = k_3 = 0.0$. It is easy to find from Eq. (7) that the first and second Hopf bifurcation frequencies are $\delta_{01} = 1.28038$ and $\delta_{02} = 0.71582$. Fig. 1 shows the variation of critical time delay τ_c with the derivative feedback gain in the (q, τ) parameter plane. The curves, which are defined by Eq. (8) and illustrated by the dotted lines and triangular lines in the figure, are indeed curves of the first and second Hopf bifurcations. These curves divide the parameter space into several regions of the stability and instability of the trivial solution. The stability and instability regions are indicated in Fig. 1 by the abbreviated terms "sts" and "uts", which stand for the stable and unstable trivial solutions, respectively. For a fixed derivative feedback gain, the trivial solution remains stable until τ reaches $\tau_{1c,0}$ corresponding to the first Hopf bifurcation, and regains its stability when τ increases to $\tau_{2c,0}$ relating to the second Hopf bifurcation. In such a way, the trivial fixed point switches its stability and instability a finite number of times, and eventually become unstable. Two curves of nonresonant Hopf bifurcations intersect at the point $(q, \tau) = (-0.40219, 5.46397)$, where time delay τ has the same value on the two curves. The points of intersection of the two curves are usually referred to as the co-dimension two bifurcation points and can be a source of more complicated dynamics.

It was numerically found that the system defined by Eq. (3) may also possess points of intersection of resonant Hopf–Hopf bifurcations. For example, two-to-one resonances of Hopf–Hopf interactions may

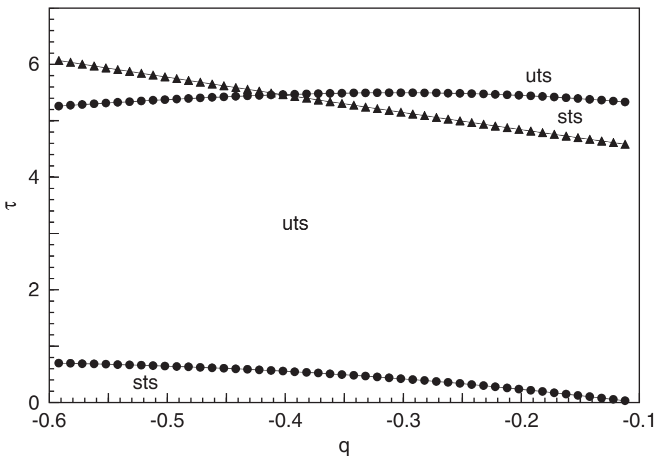

Fig. 1. Region of stability and instability of the trivial equilibrium for the case of a double Hopf bifurcation. The dotted lines represent the first Hopf bifurcations and the triangular lines stand for the second Hopf bifurcations.

appear at the point $(q,\tau)=(-0.269, 2.45595)$ for a set of the system parameters given by $\mu=0.005$, $\omega=2.1$, $p=-2.6$. The frequencies of two Hopf bifurcations were numerically found from Eq. (7) to be $\delta_{01}=2.66591$, $\delta_{02}=1.33614$, respectively. The ratio of these two frequencies is given by $\delta_{01}:\delta_{02}=1.99522$, which is nearly equal to 2. The point of intersection of two Hopf bifurcations occurs at $\tau_{1c,1}=\tau_{2c,0}$. More complicated behaviour may be expected at such a point of resonant co-dimension two bifurcations. A two-to-one resonant Hopf–Hopf interaction occurring in the controlled system will be the topic of future research.

3. Construction of the centre manifold

For simplicity, it is assumed that an intersection of nonresonant Hopf bifurcations occurs at the point (p_0, q_0, τ_0), where Eq. (4) has two pairs of purely imaginary roots $\pm i\delta_{01}$, $\pm i\delta_{02}$, and all other roots have negative real parts. In order to study the periodic solutions resulting from an interaction of two Hopf bifurcations in the neighbourhood of the bifurcation point (p_0, q_0, τ_0), three small perturbation parameters (namely, α_1, α_2 and α_3) are introduced in terms of $p=p_0+\alpha_1$, $q=q_0+\alpha_2$, $\tau=\tau_0+\alpha_3$. These perturbation parameters can easily account for the small variations of the linear feedback gains and time delay. At this stage, the perturbation parameters act as three dummy unfolding parameters. It will be shown that these dummy perturbation parameters determine two unfolding parameters in the normal forms of the nonresonant co-dimension two bifurcation.

Introducing the three dummy parameters defined above and letting $y_1=x$, $y_2=\dot{x}$ in Eq. (3) yields the following two first-order equations

$$\begin{aligned} \dot{y}_1 &= y_2, \\ \dot{y}_2 &= -\omega^2 y_1 + \mu y_2 + p_0 y_1(t-\tau) + q_0 y_2(t-\tau) + f_\alpha(y(\tau)) - f_t(y) + f_\tau(y(\tau)), \end{aligned} \tag{10}$$

where $y_1(t)$ and $y_2(t)$ have been written here as y_1 and y_2 for simplicity,

$$\begin{aligned} f_\alpha(y(\tau)) &= \alpha_1 y_1(t-\tau) + \alpha_2 y_2(t-\tau), \quad f_t(y) = \beta y_1^2 y_2 + \alpha y_1^3, \\ f_\tau(y(\tau)) &= k_1 y_1^3(t-\tau) + k_2 y_2^3(t-\tau) + k_3 y_1^2(t-\tau) y_2(t-\tau) + k_4 y_1(t-\tau) y_2^2(t-\tau). \end{aligned}$$

By normalizing time in the units of the delay in terms of $t=\bar{t}\tau$ with $\tau=\tau_0+\alpha_3$, Eq. (10) may be rewritten in the following form (which explicitly involves the three dummy unfolding parameters)

$$y_1' = \tau_0 y_2 + \alpha_3 y_2,$$

$$y_2' = -\omega^2\tau_0 y_1 + \mu\tau_0 y_2 + p_0\tau_0 y_1(t-1) + q_0\tau_0 y_2(t-1) - \alpha_3\omega^2 y_1 + \alpha_3\mu y_2 + \alpha_3 p_0 y_1(t-1) + \alpha_3 q_0 y_2(t-1) + (\tau_0+\alpha_3)[f_\alpha(y(1)) - f_t(y) + f_\tau(y(1))], \tag{11}$$

where $f_t(y) = \beta y_1^2 y_2 + \alpha y_1^3$,

$$f_\alpha(y(1)) = \alpha_1 y_1(t-1) + \alpha_2 y_2(t-1),$$

$$f_\tau(y(1)) = k_1 y_1^3(t-1) + k_2 y_2^3(t-1) + k_3 y_1^2(t-1) y_2(t-1) + k_4 y_1(t-1) y_2^2(t-1)$$

and a prime indicates the differentiation with respect to the new time $\bar{t}$ whose above bar has been removed here for brevity. For the perturbation system defined by Eq. (11), the two Hopf bifurcation frequencies, namely δ_1 and δ_2, are now given by $\delta_1 = \tau_0\delta_{01}$, $\delta_2 = \tau_0\delta_{02}$.

By letting $\dot{y}(t) = [y_1', y_2']^{\mathrm{T}}$, $y(t) = [y_1, y_2]^{\mathrm{T}}$, $y(t-1) = [y_1(t-1), y_2(t-1)]^{\mathrm{T}}$, where the superscript "T" denotes the transpose, Eq. (11) can be re-written as

$$\dot{y}(t) = L_0 y(t) + L_1 y(t-1) + [f_0(y(t)) + f_1(y(t-1))], \tag{12}$$

where

$$L_0 = \begin{bmatrix} 0 & \tau_0 \\ -\tau_0\omega^2 & \tau_0\mu \end{bmatrix}, \quad L_1 = \begin{bmatrix} 0 & 0 \\ \tau_0 p_0 & \tau_0 q_0 \end{bmatrix},$$

$$f_0(y(t)) = \begin{bmatrix} \alpha_3 y_2 \\ -\alpha_3\omega^2 y_1 + \alpha_3\mu y_2 - (\tau_0+\alpha_3) f_t(y) \end{bmatrix},$$

$$f_1(y(t-1)) = \begin{bmatrix} 0 \\ \alpha_3 p_0 y_1(t-1) + \alpha_3 q_0 y_2(t-1) + (\tau_0+\alpha_3)[f_\alpha(y(1)) + f_\tau(y(1))] \end{bmatrix}.$$

Let $B = C([-1,0], R^2)$, $L : B \to R^2$ be a continuous linear operator and $G(y_t) : R^2 \to R^2$ be a nonlinear smooth operator, then Eq. (12) can be expressed as an abstract form on the Banach space

$$\dot{y}(t) = Ly_t + G(y_t), \tag{13}$$

where $y_t \in B$ is defined by the shift of time as $y_t(\theta) = y(t+\theta)$ with $\theta \in [-1,0]$. The linear operator may be expressed in integral form as

$$L\phi = \int_{-1}^{0} [\mathrm{d}\eta(\theta)]\phi(\theta),$$

where ϕ is a given function on the space B, $\eta : [-1,0] \to R^2$ is a 2×2 matrix-valued function with bounded variation and is continuous in θ on $[-1,0)$. The function η of bounded variation in the definition of L is given by $\eta(\theta) = 0$ for $\theta \geqslant 0$, $= L_0$ for $-1 < \theta < 0$, $= L_0 + L_1$ for $\theta \leqslant -1$ [23,24].

The nonlinear smooth operator $G(y_t)$ can be defined by

$$G(y_t)(\theta) = \begin{cases} 0, & \theta \in [-1,0), \\ f_0(y(t)) + f_\tau(y(t-1)), & \theta = 0. \end{cases}$$

The infinitesimal generator A of the continuous semi-flow generated by the linear operator in Eq. (13) assumes the form

$$A\phi(\theta) = \begin{cases} \mathrm{d}\phi(\theta)/\mathrm{d}\theta, & \theta \in [-1,0), \\ L_0\phi(0) + L_1\phi(-1), & \theta = 0. \end{cases} \tag{14}$$

Let P be the invariant space for the infinitesimal generator A associated with two pairs of purely imaginary eigenvalues, $\pm i\delta_1$, $\pm i\delta_2$. In accordance with the decomposition theorem (Chapter 7 in Ref. [24]), the space B can be split into two disjoint subspaces P, Q as $B = P \oplus Q$, where Q is the complimentary subspace spanned by the eigenvalues with negative real parts. The centre subspace P of the associated linear problem can be spanned by the real and imaginary parts of the complex eigenvectors $\phi(\theta)$. The basis matrix $\Phi(\theta)$ for the space

P is found to be

$$\Phi(\theta) = (\phi_1, \phi_2, \phi_3, \phi_4) = \begin{pmatrix} \cos(\delta_1\theta) & \sin(\delta_1\theta) & \cos(\delta_2\theta) & \sin(\delta_2\theta) \\ -\delta_{01}\sin(\delta_1\theta) & \delta_{01}\cos(\delta_1\theta) & -\delta_{02}\sin(\delta_2\theta) & \delta_{02}\cos(\delta_2\theta) \end{pmatrix} \quad (15)$$

such that the matrix satisfies $\mathrm{d}\Phi/\mathrm{d}\theta = \Phi J$, where

$$J = \begin{bmatrix} 0 & \delta_1 & 0 & 0 \\ -\delta_1 & 0 & 0 & 0 \\ 0 & 0 & 0 & \delta_2 \\ 0 & 0 & -\delta_2 & 0 \end{bmatrix}.$$

Let $B^1 = C([0,1], R^2)$, and $\psi(s)$ be a row-valued generalized eigenfunction of the adjoint operator of A. The adjoint bilinear form on $B \times B^1$ is defined by [25]

$$(\psi, \phi) = \psi(0)\phi(0) - \int_{-1}^{0} \psi(s+1) L_1 \phi(s)\,\mathrm{d}s. \quad (16)$$

The basis $\Psi(s) = \mathrm{col}(\psi_1, \psi_2, \psi_3, \psi_4)$ for the dual space in B^1 can be explicitly obtained using $\Psi = (\Phi^{\mathrm{T}}, \Phi)^{-1}\Phi^{\mathrm{T}}$, so that (Ψ, Φ) is a 4×4 identity matrix.

The function $(\Phi^{\mathrm{T}}, \Phi)$ can be obtained based on the bilinear relation of the inner product matrix

$$(\Phi^{\mathrm{T}}, \Phi) = \begin{pmatrix} (\phi_1^{\mathrm{T}}, \phi_1) & (\phi_1^{\mathrm{T}}, \phi_2) & (\phi_1^{\mathrm{T}}, \phi_3) & (\phi_1^{\mathrm{T}}, \phi_4) \\ (\phi_2^{\mathrm{T}}, \phi_1) & (\phi_2^{\mathrm{T}}, \phi_2) & (\phi_2^{\mathrm{T}}, \phi_3) & (\phi_2^{\mathrm{T}}, \phi_4) \\ (\phi_3^{\mathrm{T}}, \phi_1) & (\phi_3^{\mathrm{T}}, \phi_2) & (\phi_3^{\mathrm{T}}, \phi_3) & (\phi_3^{\mathrm{T}}, \phi_4) \\ (\phi_4^{\mathrm{T}}, \phi_1) & (\phi_4^{\mathrm{T}}, \phi_2) & (\phi_4^{\mathrm{T}}, \phi_3) & (\phi_4^{\mathrm{T}}, \phi_4) \end{pmatrix} = \begin{pmatrix} a_{11} & a_{12} & a_{13} & a_{14} \\ a_{21} & a_{22} & a_{23} & a_{24} \\ a_{31} & a_{32} & a_{33} & a_{34} \\ a_{41} & a_{42} & a_{43} & a_{44} \end{pmatrix}, \quad (17)$$

where $a_{11} = \frac{1}{2}(2 - \mu\delta_{01}^2\tau_0 - q_0\delta_{01}\sin\delta_1)$,

$$a_{12} = \tfrac{1}{2}(\delta_{01}^3\tau_0 - \delta_{01}\tau_0\omega^2 + p_0\sin\delta_1),$$

$$a_{13} = \frac{1}{\delta_1^2 - \delta_2^2}[q_0\delta_{01}\delta_2(\delta_2\sin\delta_1 - \delta_1\sin\delta_2) + p_0(\cos\delta_1 - \cos\delta_2)\delta_1^2 + \delta_1^2 - \delta_2^2],$$

$$a_{14} = \frac{1}{\delta_1^2 - \delta_2^2}[p_0\delta_1(\delta_1\sin\delta_2 - \delta_2\sin\delta_1) + (\cos\delta_1 - \cos\delta_2)q_0\delta_1^2\delta_{02}],$$

$$a_{21} = \tfrac{1}{2}(\delta_{01}\tau_0\omega^2 - \delta_{01}^3\tau_0 + p_0\sin\delta_1),$$

$$a_{22} = \tfrac{1}{2}(2\delta_{01}^2 - \mu\delta_{01}^2\tau_0 + q_0\delta_{01}\sin\delta_1)$$

and the other 10 coefficients a_{23}–a_{44} are not given in the present paper for clarity.

It is found after performing some algebraic manipulations that the basis $\Psi(0)$ to be needed for the subsequent analysis can be given by

$$\Psi(0) = \begin{bmatrix} b_{11} & b_{12} \\ b_{21} & b_{22} \\ b_{31} & b_{32} \\ b_{41} & b_{42} \end{bmatrix}, \quad (18)$$

where $b_{11} = d_{11} + d_{13}$, $b_{12} = \delta_{01}d_{12} + \delta_{02}d_{14}$, $b_{21} = d_{21} + d_{23}$, $b_{22} = \delta_{01}d_{22} + \delta_{02}d_{24}$, $b_{31} = d_{31} + d_{33}$, $b_{32} = \delta_{01}d_{32} + \delta_{02}d_{34}$, $b_{41} = d_{41} + d_{43}$, $b_{42} = \delta_{01}d_{42} + \delta_{02}d_{44}$ with

$$
\begin{aligned}
d_{11} &= \frac{1}{\Delta}(a_{23}a_{34}a_{42} - a_{24}a_{33}a_{42} + a_{24}a_{32}a_{43} - a_{22}a_{34}a_{43} + a_{22}a_{33}a_{44} - a_{23}a_{32}a_{44}),\\
d_{12} &= \frac{1}{\Delta}(a_{14}a_{33}a_{42} - a_{13}a_{34}a_{42} + a_{12}a_{34}a_{43} - a_{14}a_{32}a_{43} + a_{13}a_{32}a_{44} - a_{12}a_{33}a_{44}),\\
d_{13} &= \frac{1}{\Delta}(a_{13}a_{24}a_{42} - a_{14}a_{23}a_{42} + a_{14}a_{22}a_{43} - a_{12}a_{24}a_{43} + a_{12}a_{23}a_{44} - a_{13}a_{22}a_{44}),\\
d_{14} &= \frac{1}{\Delta}(a_{14}a_{23}a_{32} - a_{13}a_{24}a_{32} + a_{12}a_{24}a_{33} - a_{14}a_{22}a_{33} + a_{13}a_{22}a_{34} - a_{12}a_{23}a_{34}),
\end{aligned}
$$

the symbol Δ stands for the determinant of the matrix $(\Phi^{\mathrm{T}}, \Phi)$ given by Eq. (17), and the other 12 coefficients, $d_{21}-d_{44}$, are not given here for brevity.

The centre manifold theorem assumes that the dynamic behaviour of orbits of Eq. (13) in B at the origin can be split into stable and centre manifolds. The flow on the centre manifold, which is tangent to the invariant space P associated with two pairs of purely imaginary eigenvalues, is given by $y_t = \Phi z(t) + h(z(t); F)$, where $z(t) = (z_1, z_2, z_3, z_4)^{\mathrm{T}}$, $h(z; F) \in Q$ for each z and is a C^{r-1} function of z. In terms of the coordinates, z, the solution of Eq. (13), y_t, can be expressed as

$$
\begin{aligned}
\begin{pmatrix} y_1(t) \\ y_2(t) \end{pmatrix} &= \begin{pmatrix} z_1 + z_3 \\ z_2\delta_{01} + z_4\delta_{02} \end{pmatrix},\\
\begin{pmatrix} y_1(t-1) \\ y_2(t-1) \end{pmatrix} &= \begin{pmatrix} z_1 \cos \delta_1 - z_2 \sin \delta_1 + z_3 \cos \delta_2 - z_4 \sin \delta_2 \\ z_1\delta_{01} \sin \delta_1 + z_2\delta_{01} \cos \delta_1 + z_3\delta_{02} \sin \delta_2 + z_4\delta_{02} \cos \delta_2 \end{pmatrix}.
\end{aligned} \tag{19}
$$

The local coordinates on the centre manifold are given by the following 4D ordinary differential equations:

$$
\dot{z} = Jz + \Psi(0)G(\Phi z + h(z, F)). \tag{20}
$$

Substitution of Eqs. (18) and (19) in Eq. (20) gives rise to

$$
\dot{z} = \begin{bmatrix} l_{11} & \delta_1 + l_{12} & l_{13} & l_{14} \\ -\delta_1 + l_{21} & l_{22} & l_{23} & l_{24} \\ l_{31} & l_{32} & l_{33} & \delta_2 + l_{34} \\ l_{41} & l_{42} & -\delta_2 + l_{43} & l_{44} \end{bmatrix} \begin{pmatrix} z_1 \\ z_2 \\ z_3 \\ z_4 \end{pmatrix} + \begin{bmatrix} b_{12} \\ b_{22} \\ b_{32} \\ b_{42} \end{bmatrix} \mathrm{NLT}, \tag{21}
$$

where the term NLT represents the nonlinear terms, $l_{i1} = b_{i2}b_{210}$, $l_{i2} = b_{i1}b_{120} + b_{i2}b_{220}$, $l_{i3} = b_{i2}b_{230}$, $l_{i4} = b_{i1}b_{140} + b_{i2}b_{240}$, $i = 1, 2, 3, 4$ with $b_{120} = \alpha_3\delta_{01}$, $b_{140} = \alpha_3\delta_{02}$,

$$
\begin{aligned}
b_{210} &= -\alpha_3\omega^2 + (\alpha_1\tau_0 + \alpha_3 p_0 + \alpha_1\alpha_3)\cos \delta_1 + (\alpha_2\delta_{01}\tau_0 + \alpha_3\delta_{01}q_0 + \alpha_2\alpha_3\delta_{01})\sin \delta_1,\\
b_{220} &= \mu\alpha_3\delta_{01} + (\alpha_2\delta_{01}\tau_0 + q_0\alpha_3\delta_{01} + \alpha_2\alpha_3\delta_{01})\cos \delta_1 - (\tau_0\alpha_1 + p_0\alpha_3 + \alpha_1\alpha_3)\sin \delta_1,\\
b_{230} &= -\alpha_3\omega^2 + (\alpha_1\tau_0 + \alpha_3 p_0 + \alpha_1\alpha_3)\cos \delta_2 + (\alpha_2\delta_2 + \alpha_3\delta_{02}q_0 + \alpha_2\alpha_3\delta_{02})\sin \delta_2,\\
b_{240} &= \mu\alpha_3\delta_{02} + (\alpha_2\delta_2 + q_0\alpha_3\delta_{02} + \alpha_2\alpha_3\delta_{02})\cos \delta_2 - (\tau_0\alpha_1 + p_0\alpha_3 + \alpha_1\alpha_3)\sin \delta_2.
\end{aligned}
$$

The nonlinear function, NLT, which consists of 20 terms of the third order, is given by

$$
\begin{aligned}
\mathrm{NLT} = {} & a_{111}z_1^3 + a_{112}z_1^2 z_2 + a_{113}z_1^2 z_3 + a_{114}z_1^2 z_4 + a_{122}z_1 z_2^2 + a_{123}z_1 z_2 z_3 + a_{124}z_1 z_2 z_4\\
& + a_{133}z_1 z_3^2 + a_{134}z_1 z_3 z_4 + a_{144}z_1 z_4^2 + a_{222}z_2^3 + a_{223}z_2^2 z_3 + a_{224}z_2^2 z_4 + a_{233}z_2 z_3^2\\
& + a_{234}z_2 z_3 z_4 + a_{244}z_2 z_4^2 + a_{333}z_3^3 + a_{334}z_3^2 z_4 + a_{344}z_3 z_4^2 + a_{444}z_4^3,
\end{aligned} \tag{22}
$$

where $a_{111} = (\tau_0 + \alpha_3)[-\alpha + k_1 \cos^3 \delta_1 + k_2\delta_{01}^3 \sin^3 \delta_1 + (k_3 + k_4)\delta_{01} \sin \delta_1 \cos^2 \delta_1]$, the other 19 coefficients $a_{112}-a_{444}$ can also be expressed in terms of the system parameters and two Hopf bifurcation frequencies as well as the corresponding critical time delay. For brevity, they are not reproduced here.

4. Solutions of co-dimension two bifurcation and their stability

The solutions of Eq. (21) will be approximately obtained using the method of multiple scales [26,27]. The dynamic behaviour of the system in the neighbourhood of the point of the nonresonant co-dimension two bifurcation will be studied based on a set of four averaged equations that determine the amplitudes and phases of the bifurcating periodic solutions. Eq. (21) can be rewritten in the component form as

$$\begin{aligned}\dot{z}_1 &= l_{11}z_1 + (\delta_1 + l_{12})z_2 + l_{13}z_3 + l_{14}z_4 + f_{10}(z),\\ \dot{z}_2 &= (-\delta_1 + l_{21})z_1 + l_{22}z_2 + l_{23}z_3 + l_{24}z_4 + f_{20}(z),\\ \dot{z}_3 &= l_{31}z_1 + l_{32}z_2 + l_{33}z_3 + (\delta_2 + l_3)z_4 + f_{30}(z),\\ \dot{z}_4 &= l_{41}z_1 + l_{42}z_2 + (-\delta_2 + l_{43})z_3 + l_{44}z_4 + f_{40}(z),\end{aligned} \tag{23}$$

where $f_{10}(z) = b_{12}\mathrm{NLT}, f_{20}(z) = b_{22}\mathrm{NLT}, f_{30}(z) = b_{32}\mathrm{NLT}, f_{40}(z) = b_{42}\mathrm{NLT}$.

It is assumed that the solutions of Eq. (23) in the neighbourhood of the trivial equilibrium are represented by an expansion of the form

$$z_i(t;\varepsilon) = \varepsilon^{1/2}z_{i1}(T_0, T_1, \ldots) + \varepsilon^{3/2}z_{i2}(T_0, T_1, \ldots) + \cdots \quad (i = 1, 2, 3, 4). \tag{24}$$

where ε is a non-dimensional small parameter, and the new multiple independent variables of time are introduced according to $T_k = \varepsilon^k t$, $k = 0, 1, 2, \ldots$. It follows that the derivatives with respect to t now become expansions in terms of the partial derivatives with respect to T_k given by

$$\frac{\mathrm{d}}{\mathrm{d}t} = \frac{\mathrm{d}T_0}{\mathrm{d}t}\frac{\partial}{\partial T_0} + \frac{\mathrm{d}T_1}{\mathrm{d}t}\frac{\partial}{\partial T_1} + \frac{\mathrm{d}T_2}{\mathrm{d}t}\frac{\partial}{\partial T_2} + \cdots = D_0 + \varepsilon D_1 + \varepsilon^2 D_2 + \cdots, \tag{25}$$

where the differentiation operator $D_k = \partial/\partial T_k$.

Substituting the approximate solutions (24) into Eq. (23) and then balancing the like powers of ε results in the following ordered perturbation equations:

$$\varepsilon^{1/2}: D_0 z_{11} = \delta_1 z_{21}, \tag{26}$$

$$D_0 z_{21} = -\delta_1 z_{11}, \tag{27}$$

$$D_0 z_{31} = \delta_2 z_{41}, \tag{28}$$

$$D_0 z_{41} = -\delta_2 z_{31}, \tag{29}$$

$$\varepsilon^{3/2}: \quad D_0 z_{12} = g_{11}(z_{11}, z_{21}, z_{31}, z_{41}) + \delta_1 z_{22} - D_1 z_{11} + f_{11}(z_{11}, z_{21}, z_{31}, z_{41}), \tag{30}$$

$$D_0 z_{22} = g_{21}(z_{11}, z_{21}, z_{31}, z_{41}) - \delta_1 z_{12} - D_1 z_{21} + f_{21}(z_{11}, z_{21}, z_{31}, z_{41}) \tag{31}$$

$$D_0 z_{32} = g_{31}(z_{11}, z_{21}, z_{31}, z_{41}) + \delta_2 z_{42} - D_1 z_{31} + f_{31}(z_{11}, z_{21}, z_{31}, z_{41}), \tag{32}$$

$$D_0 z_{42} = g_{41}(z_{11}, z_{21}, z_{31}, z_{41}) - \delta_2 z_{32} - D_1 z_{41} + f_{41}(z_{11}, z_{21}, z_{31}, z_{41}), \tag{33}$$

where $D_0 = \partial/\partial T_0$, $D_1 = \partial/\partial T_1$, the coefficients of the perturbation linear terms l_{ij} in Eq. (23) have been rescaled in terms of $l_{ij} = \varepsilon\bar{l}_{ij}$ and the overbars in $\bar{l}_{ij}$ have been removed for brevity. The four linear functions of $z_{i1}(i = 1, 2, 3, 4)$, namely g_{11}, g_{21}, g_{31} and g_{41}, are given by

$$\begin{aligned}g_{11} &= l_{11}z_{11} + l_{12}z_{21} + l_{13}z_{31} + l_{14}z_{41}, \quad g_{21} = l_{21}z_{11} + l_{22}z_{21} + l_{23}z_{31} + l_{24}z_{41},\\ g_{31} &= l_{31}z_{11} + l_{32}z_{21} + l_{33}z_{31} + l_{34}z_{41}, \quad g_{41} = l_{41}z_{11} + l_{42}z_{21} + l_{43}z_{31} + l_{44}z_{41}\end{aligned}$$

and the f_{i1} are nonlinear functions of $z_{i1}(i = 1, 2, 3, 4)$ which have been solved from the perturbation Eqs. (26)–(29).

Differentiating Eqs. (26) and (28) and substituting Eqs. (27) and (29) into the resulting equations yields two second-order ordinary differential equations

$$D_0^2 z_{11} + \delta_1^2 z_{11} = 0, \tag{34}$$

$$D_0^2 z_{31} + \delta_2^2 z_{31} = 0. \tag{35}$$

The solutions of Eqs. (34) and (35) can be written in a general form as

$$z_{11} = r_1(T_1)\cos[\delta_1 T_0 + \phi_1(T_1)] \equiv r_1 \cos\theta_1, \tag{36}$$

$$z_{31} = r_2(T_1)\cos[\delta_2 T_0 + \phi_2(T_1)] \equiv r_2 \cos\theta_2, \tag{37}$$

where r_1, r_2, ϕ_1, ϕ_2 represent, respectively, the amplitudes and phases of the bifurcating periodic solutions. The solutions, z_{21} and z_{41}, which can be directly obtained by Eqs. (26) and (28), are given by

$$z_{21} = -r_1 \sin(\delta_1 T_0 + \phi_1) = -r_1 \sin\theta_1, \tag{38}$$

$$z_{41} = -r_2 \sin(\delta_2 T_0 + \phi_2) = -r_2 \sin\theta_2. \tag{39}$$

Note that solutions (36)–(39) imply that $D_0 r_1 = D_0 r_2 = 0$, and $D_0\phi_1 = D_0\phi_2 = 0$.

Similarly, differentiating Eqs. (30) and (32) and then substituting Eqs. (31) and (33) into the resultant equations results in

$$D_0^2 z_{12} + \delta_1^2 z_{12} = D_0 g_{11} - D_0 D_1 z_{11} + D_0 f_{11} + \delta_1 g_{21} - \delta_1 D_1 z_{21} + \delta_1 f_{21}, \tag{40}$$

$$D_0^2 z_{32} + \delta_2^2 z_{32} = D_0 g_{31} - D_0 D_1 z_{31} + D_0 f_{31} + \delta_2 g_{41} - \delta_2 D_1 z_{41} + \delta_2 f_{41}. \tag{41}$$

Substituting solutions (36)–(39) into the right-hand sides of Eqs. (40)–(41) and then eliminating the possible secular terms which may appear in the solutions of z_{12} and z_{32}, gives $D_1 r_1$, $D_1 r_2$, $D_1\phi_1$ and $D_1\phi_2$ as

$$\begin{aligned} D_1 r_1 &= \mu_1 r_1 + s_{11} r_1^3 + s_{12} r_1 r_2^2,\\ D_1 r_2 &= \mu_2 r_2 + s_{21} r_1^2 r_2 + s_{22} r_2^3,\\ D_1\phi_1 &= \rho_1 + s_{31} r_1^2 + s_{32} r_2^2,\\ D_1\phi_2 &= \rho_2 + s_{41} r_1^2 + s_{42} r_2^2, \end{aligned} \tag{42}$$

where $\mu_1 = 1/2(l_{11} + l_{22})$, $\mu_2 = 1/2(l_{33} + l_{44})$,

$$\begin{aligned} s_{11} &= \tfrac{1}{8}(3a_{111}b_{12} + a_{122}b_{12} + a_{112}b_{22} + 3a_{222}b_{22}),\\ s_{12} &= \tfrac{1}{4}(a_{133}b_{12} + a_{144}b_{12} + a_{233}b_{22} + a_{244}b_{22}),\\ s_{21} &= \tfrac{1}{4}(a_{113}b_{32} + a_{223}b_{32} + a_{114}b_{42} + a_{224}b_{42}),\\ s_{22} &= \tfrac{1}{8}(3a_{333}b_{32} + a_{344}b_{32} + a_{334}b_{42} + 3a_{344}b_{42}),\\ \rho_1 &= \tfrac{1}{2}(l_{12} - l_{21}), \rho_2 = \tfrac{1}{2}(l_{34} - l_{43}),\\ s_{31} &= \tfrac{1}{8}(a_{112}b_{12} + 3a_{222}b_{12} - 3a_{111}b_{22} - a_{122}b_{22}),\\ s_{32} &= \tfrac{1}{4}(a_{233}b_{12} + a_{244}b_{12} - a_{133}b_{22} - a_{144}b_{22}),\\ s_{41} &= \tfrac{1}{4}(a_{114}b_{32} + a_{224}b_{32} - a_{113}b_{42} - a_{223}b_{42}),\\ s_{42} &= \tfrac{1}{8}(a_{334}b_{32} + 3a_{344}b_{32} - 3a_{333}b_{42} - a_{344}b_{42}). \end{aligned}$$

The averaged equations that determine the amplitudes and phases of the bifurcating periodic solutions can be written as

$$\begin{aligned} \frac{dr_1}{dt} &= \frac{\partial r_1}{\partial T_0}\frac{\partial T_0}{\partial t} + \frac{\partial r_1}{\partial T_1}\frac{\partial T_1}{\partial t} = D_0 r_1 + \varepsilon D_1 r_1 = D_1 r_1,\\ \frac{d\phi_1}{dt} &= \frac{\partial \phi_1}{\partial T_0}\frac{\partial T_0}{\partial t} + \frac{\partial \phi_1}{\partial T_1}\frac{\partial T_1}{\partial t} = D_0 \phi_1 + \varepsilon D_1 \phi_1 = D_1 \phi_1,\\ \frac{dr_2}{dt} &= \frac{\partial r_2}{\partial T_0}\frac{\partial T_0}{\partial t} + \frac{\partial r_2}{\partial T_1}\frac{\partial T_1}{\partial t} = D_0 r_2 + \varepsilon D_1 r_2 = D_1 r_2,\\ \frac{d\phi_2}{dt} &= \frac{\partial \phi_2}{\partial T_0}\frac{\partial T_0}{\partial t} + \frac{\partial \phi_2}{\partial T_1}\frac{\partial T_1}{\partial t} = D_0 \phi_2 + \varepsilon D_1 \phi_2 = D_1 \phi_2, \end{aligned} \tag{43}$$

where it has been set that $\varepsilon = 1$.

Based on Eq. (43), the explicit formulae of the normal forms of the nonresonant co-dimension two bifurcation of Hopf–Hopf interactions are expressed as

$$\dot{r}_1 = -\mu_1 r_1 + s_{11} r_1^3 + s_{12} r_1 r_2^2, \tag{44}$$

$$\dot{r}_2 = -\mu_2 r_2 + s_{21} r_1^2 r_2 + s_{22} r_2^3, \tag{45}$$

$$\dot{\theta}_1 = \delta_1 + \rho_1 + s_{31} r_1^2 + s_{32} r_2^2, \tag{46}$$

$$\dot{\theta}_2 = \delta_2 + \rho_2 + s_{41} r_1^2 + s_{42} r_2^2. \tag{47}$$

The two unfolding parameters, μ_1 and μ_2, are reproduced here in terms of the three dummy parameters as

$$\mu_1 = h_{11}\alpha_1 + h_{12}\alpha_2 + h_{13}\alpha_3,$$
$$\mu_2 = h_{21}\alpha_1 + h_{22}\alpha_2 + h_{23}\alpha_3,$$

where

$$h_{11} = -\frac{\tau_0}{2}(b_{12}\cos\delta_1 - b_{22}\sin\delta_1), \quad h_{12} = -\frac{\delta_1}{2}(b_{12}\sin\delta_1 + b_{22}\cos\delta_1),$$

$$h_{13} = \tfrac{1}{2}\big[b_{12}(\omega^2 - p_0\cos\delta_1 - q_0\delta_{01}\sin\delta_1) - b_{21}\delta_{01} - b_{22}(\mu\delta_{01} - p_0\sin\delta_1 + q_0\delta_{01}\cos\delta_1)\big],$$

$$h_{21} = -\frac{\tau_0}{2}(b_{32}\cos\delta_2 - b_{42}\sin\delta_2), \quad h_{22} = -\frac{\delta_2}{2}(b_{32}\sin\delta_2 + b_{42}\cos\delta_2),$$

$$h_{23} = \tfrac{1}{2}\big[b_{32}(\omega^2 - p_0\cos\delta_2 - q_0\delta_{02}\sin\delta_2) - b_{41}\delta_{02} - b_{42}(\mu\delta_{02} - p_0\sin\delta_2 + q_0\delta_{02}\cos\delta_2)\big].$$

It is shown that the two unfolding parameters are characterized by the system parameters and dummy perturbation parameters. The derivation of the unfolding parameters distinguishes from the existing work [16], where the universal unfolding was given based on the normal forms of the degenerate system. Merits of the unfolding parameters obtained here are two-fold. First of all, it is easy to locate the region of the dummy perturbation parameters where the different behaviour may appear in the vicinity of the co-dimension two bifurcation. The analytically obtained values of the dummy perturbation parameters can be served as a guide to perform the numerical integration of the original equation. The results of numerical integration can be in turn used to validate the analytical predictions. Second, due to the fact that the unfolding parameters are closely related to the physical perturbation parameters, the effect of variations of the controlled parameters on the observed behaviour of the controlled system can be easily studied by simply changing the values of the dummy parameters on the boundary of the stability region of the fixed point.

The behaviour of a similar system to that defined by Eqs. (44)–(47) has been studied by considering 12 different cases, depending on the values of the unfolding parameters and cubic coefficients [28]. The detailed bifurcations and dynamics for each case are not reproduced here in the unfolding parameters (μ_1, μ_2) plane. In the next section, the steady-state solutions and their stability will be studied and interpreted by illustrative examples in terms of the dummy perturbation parameters (α_1, α_2). Here, the dynamics of Eqs. (44)–(47) is understood by finding the fixed points and studying the nature of their stability. The fixed points are obtained by setting $\dot{r}_1 = \dot{r}_2 = 0$ in Eqs. (44) and (45). It is easy to note that $(r_1, r_2) = (0, 0)$ is always an equilibrium and that up to three other equilibria can appear as follows:

$$(r_1, r_2) = \left(\sqrt{\frac{\mu_1}{s_{11}}}, 0\right) \quad \text{for } \frac{\mu_1}{s_{11}} > 0,$$

$$(r_1, r_2) = \left(0, \sqrt{\frac{\mu_2}{s_{22}}}\right) \quad \text{for } \frac{\mu_2}{s_{22}} > 0,$$

$$(r_1, r_2) = \left(\sqrt{\frac{s_{12}\mu_2 - s_{22}\mu_1}{s_{12}s_{21} - s_{11}s_{22}}}, \sqrt{\frac{s_{21}\mu_1 - s_{11}\mu_2}{s_{12}s_{21} - s_{11}s_{22}}}\right) \quad \text{for } \frac{s_{12}\mu_2 - s_{22}\mu_1}{s_{12}s_{21} - s_{11}s_{22}} > 0, \frac{s_{21}\mu_1 - s_{11}\mu_2}{s_{12}s_{21} - s_{11}s_{22}} > 0. \tag{48}$$

For simplicity, the above solutions will be referred to here as solutions S1, S2, S3 and S4, respectively. In particular, solution S1 is the initial equilibrium of the corresponding autonomous system. Solution S2 is the periodic solution with the frequency resulting from the first Hopf bifurcation, which is given by

$$\omega_{H1} = \delta_1 + \rho_1 + \frac{\mu_1 s_{31}}{s_{11}}. \tag{49}$$

Solution S3 is the periodic solution resulting from the second Hopf bifurcation with the frequency being

$$\omega_{H2} = \delta_2 + \rho_2 + \frac{\mu_2 s_{42}}{s_{22}}. \tag{50}$$

Solution S4 is a quasi-periodic motion with two frequencies of an irrational ratio being

$$\omega_{H1} = \delta_1 + \rho_1 + \frac{(s_{21}s_{32} - s_{22}s_{31})\mu_1 + (s_{12}s_{31} - s_{11}s_{32})\mu_2}{s_{12}s_{21} - s_{11}s_{22}},$$

$$\omega_{H2} = \delta_2 + \rho_2 + \frac{(s_{21}s_{42} - s_{22}s_{41})\mu_1 + (s_{12}s_{41} - s_{11}s_{42})\mu_2}{s_{12}s_{21} - s_{11}s_{22}}. \tag{51}$$

The stability of these four solutions can be examined by studying the eigenvalues of the corresponding Jacobian matrix. The Jacobian matrix of Eqs. (44) and (45) takes the form

$$J = \begin{bmatrix} -\mu_1 + 3s_{11}r_1^2 + s_{12}r_2^2 & 2s_{12}r_1r_2 \\ 2s_{21}r_1r_2 & -\mu_2 + s_{21}r_1^2 + 3s_{22}r_2^2 \end{bmatrix}. \tag{52}$$

It is easy to find that the stability conditions for the initial equilibrium, solution S1, are

$$\mu_1 > 0, \mu_2 > 0. \tag{53}$$

The stability conditions for solution S2 are

$$\mu_1 < 0, s_{21}\mu_1 < s_{11}\mu_2. \tag{54}$$

The stability conditions for solution S3 are

$$\mu_2 < 0, s_{12}\mu_2 < s_{22}\mu_1. \tag{55}$$

The two-dimensional (2D) torus solution, solution S4, is asymptotically stable if the following two inequalities hold:

$$s_{11}r_1^2 < -s_{22}r_2^2, s_{12}s_{21} < s_{11}s_{22}. \tag{56}$$

A quasi-periodic motion on a three-dimensional (3D) torus may appear after a quasi-periodic solution on a 2D torus loses its stability via a Neimark–Sacker bifurcation. The quasi-periodic motion on a 3D torus can be viewed as a motion by adding a third periodic motion to the 2D quasi-periodic motion.

On the basis of the above analysis, it is easy to note that the possible solutions of the corresponding autonomous system in the neighbourhood of the nonresonant co-dimension two bifurcation of Hopf–Hopf interactions may be the initial equilibrium solution, the first Hopf bifurcation solution with frequency ω_{H1}, the second Hopf bifurcation solution with frequency ω_{H2}, a 2D torus solution with frequencies ω_{H1} and ω_{H2}, as well as the quasi-periodic solution on a 3D torus, which results from a quasi-periodic solution on a 2D torus losing its stability via a Neimark–Sacker bifurcation. The above discussion is for the general system defined by Eqs. (44)–(47). For a specific system, the dynamics of the system will be discussed numerically in the next section for a given set of the system parameters.

5. Illustrative examples

The explicit expressions for the normal forms of the nonresonant co-dimension two bifurcation of Hopf–Hopf interactions can be re-written in terms of the three dummy unfolding parameters α_1, α_2, and α_3 as

$$\dot{r}_1 = (h_{11}\alpha_1 + h_{12}\alpha_2 + h_{13}\alpha_3)r_1 + s_{11}r_1^3 + s_{12}r_1r_2^2,$$

$$\dot{r}_2 = (h_{21}\alpha_1 + h_{22}\alpha_2 + h_{23}\alpha_3)r_2 + s_{21}r_1^2 r_2 + s_{22}r_2^3,$$

$$\dot{\theta}_1 = \delta_1 + h_{31}\alpha_1 + h_{32}\alpha_2 + h_{33}\alpha_3 + s_{31}r_1^2 + s_{32}r_2^2,$$

$$\dot{\theta}_2 = \delta_2 + h_{41}\alpha_1 + h_{42}\alpha_2 + h_{43}\alpha_3 + s_{41}r_1^2 + s_{42}r_2^2, \tag{57}$$

where the six coefficients $h_{31}-h_{43}$ are determined by the system parameters and dummy perturbation parameters. For brevity, they are not reproduced here.

The solutions of Eq. (57) and their stability characteristics can be studied by a similar procedure that was developed based on Eqs. (44)–(47). It is found that the trivial equilibrium of the autonomous system may lose its stability via a supercritical or subcritical single Hopf bifurcation and regains its stability via a reverse supercritical or subcritical single Hopf bifurcation with an increase of time delay. Hence, the system defined by Eq. (3) may exhibit two types of Hopf–Hopf interactions; namely, supercritical–supercritical interactions and subcritical–subcritical interactions. As discussed in Fig. 1, for the specific system with the parameters given by $\mu = 0.1$, $\omega = 1.0$, $p = -0.4$, $\alpha = 0.4$, $\beta = 0.5$, $k_1 = 0.2$, $k_2 = k_3 = 0.0$, $k_4 = 0.5$, $q = -0.402189$, the two frequencies of nonresonant Hopf bifurcations were found to be $\delta_{01} = 1.28038$ and $\delta_{02} = 0.71582$. It was also found that the first single Hopf bifurcation is supercritical and the second single Hopf bifurcation is a reverse supercritical bifurcation. The calculation showed that a double Hopf bifurcation point occurs at $\tau_{1c,1} = \tau_{2c,0}$, as defined in Eq. (8), where two curves of the first and second Hopf bifurcations intersect at the point $(q, \tau) = (-0.402189, 5.46397)$. The point of the intersection of nonresonant Hopf bifurcations is an interaction of supercritical–supercritical Hopf bifurcations. For this specific system, Eq. (57) becomes

$$\dot{r}_1 = -(1.48776\alpha_1 + 0.454302\alpha_2)r_1 - 0.23349r_1^3 - 0.047818r_1r_2^2,$$
$$\dot{r}_2 = -(0.44829\alpha_1 + 1.38577\alpha_2)r_2 - 1.51265r_1^2r_2 - 0.693171r_2^3,$$
$$\dot{\theta}_1 = 6.99593 + 0.35482\alpha_1 - 1.9049\alpha_2 + 0.55454r_1^2 + 1.00912r_2^2,$$
$$\dot{\theta}_2 = 3.9112 + 1.93592\alpha_1 - 0.320894\alpha_2 + 1.72255r_1^2 + 0.588559r_2^2. \tag{58}$$

Here, the third dummy parameter has been set $\alpha_3 = 0.0$. If let either $\alpha_1 = 0.0$ or $\alpha_2 = 0.0$ in Eq. (57), the perturbation parameter α_3 will be involved in the resultant averaged equation and thus the influence of time delay on the behaviour of the system can be easily studied in a similar procedure.

The steady-state solutions of Eq. (58) can be easily found as follows: Solution S1, the initial equilibrium solution described by

$$r_1 = r_2 = 0.0. \tag{59}$$

Solution S2, the first Hopf bifurcation solution given by

$$r_1 = 2.06949\sqrt{-1.48776\alpha_1 - 0.454302\alpha_2}, r_2 = 0,$$

$$\omega_{H1} = 6.99593 - 3.17861\alpha_1 - 2.98386\alpha_2. \tag{60}$$

Solution S3, the second Hopf bifurcation solution determined by

$$r_1 = 0, \quad r_2 = 1.2011\sqrt{-0.44829\alpha_1 - 1.38577\alpha_2},$$

$$\omega_{H2} = 3.9112 + 1.55529\alpha_1 - 1.49752\alpha_2. \tag{61}$$

Solution S4, the quasi-periodic solution on a 2D torus with the amplitudes and frequencies being

$$r_1 = 3.3423\sqrt{-1.00984\alpha_1 - 0.248644\alpha_2}, \quad r_2 = \sqrt{23.9705\alpha_1 + 4.06213\alpha_2},$$

$$\omega_{H1} = 6.99593 + 18.2881\alpha_1 + 0.65397\alpha_2,$$
$$\omega_{H2} = 3.9112 - 9.03983\alpha_1 - 2.71464\alpha_2. \tag{62}$$

The stable region for solution S1 is

$$0.44829\alpha_1 + 1.38577\alpha_2 > 0,$$
$$1.48776\alpha_1 + 0.454302\alpha_2 > 0. \quad (63)$$

The stability conditions for solution S2 are given by

$$1.48776\alpha_1 + 0.454302\alpha_2 < 0,$$
$$4.595\alpha_1 + 0.778685\alpha_2 < 0. \quad (64)$$

It is noted that the first inequality violates the second condition given in Eq. (63) for a stable solution of S1. This suggests that solution S2 appears after solution S1 loses its stability.

The stability conditions for solution S3 are

$$0.44829\alpha_1 + 1.38577\alpha_2 < 0,$$
$$1.45684\alpha_1 + 0.358705\alpha_2 > 0. \quad (65)$$

The first inequality given by Eq. (63) is contradictory to the first condition given in Eq. (65), which suggests solution S3 bifurcating from solution S1.

The stability conditions for solution S4 can be obtained by evaluating the trace and determinant of the corresponding Jacobian matrix. Ensuring the stability of solution S4 requires

$$13.9817\alpha_1 + 2.16721\alpha_2 > 0,$$
$$(1.00984\alpha_1 + 0.248644\alpha_2)(23.9705\alpha_1 + 4.06213\alpha_2) < 0. \quad (66)$$

It is easy to note from Eq. (62) that the second inequality in Eq. (66) is automatically satisfied as long as solution S4 exists.

A careful check on the existence of solutions and their stability conditions indicates that the (α_1, α_2) parameter space can be divided into four regions. The boundaries of these regions are defined by four critical lines, namely B_1, B_2, B_3 and B_4, which are derived from Eqs. (63)–(65). These critical lines are determined by

$$B_1 : \alpha_2 = -0.323496\alpha_1, \alpha_1 > 0,$$
$$B_2 : \alpha_2 = -3.27483\alpha_1, \alpha_1 < 0,$$
$$B_3 : \alpha_2 = -4.06138\alpha_1, \alpha_1 > 0,$$
$$B_4 : \alpha_2 = -5.90097\alpha_1, \alpha_1 > 0. \quad (67)$$

The critical lines of bifurcations are illustrated in Fig. 2. A stable solution of S1 exists in the region between the lines B_1 and B_2. Crossing these two critical lines leads to solutions S2 and S3, respectively, which bifurcate from solution S1 via the appearance of a zero eigenvalue. A stable solution of S2 exists in the region between the lines B_2 and B_4, and a stable solution of S3 exists in the region between two lines B_1 and B_3. Along the critical line B_3, a secondary Hopf bifurcation solution with frequency ω_{H1} takes place from solution S3, which leads to the 2D torus solution given by Eq. (62). Similarly, a secondary Hopf bifurcation solution with frequency ω_{H2} occurs from solution S2 along the critical line B_4, which gives rise to a 2D torus solution.

The analytical predictions can be easily validated by the numerical results. By choosing a point in the parameter space as $(\alpha_1, \alpha_2) = (0.001, 0.1)$, which is located in the stable region for solution S1. The numerical solution of integration of Eq. (3) is shown in Fig. 3a. The trajectory starting from the initial conditions $(0.5, -0.5)$ asymptotically converges to the origin (i.e., solution S1). Fig. 3b shows the trajectory of solution S2, for the parameters located at $(\alpha_1, \alpha_2) = (-0.001, -0.0035)$. The amplitude and frequency of solution S2 are found from Eq. (64) to be $r_1 = 0.1148$ and $\omega_{H1} = 7.00955$. Thus, the first-order approximate solution of S2 can be written in terms of the original variables as

$$x = 0.1148 \cos(1.2829t).$$

The results of numerical integration of Eq. (3) suggest that the amplitude and frequency of the periodic solution are 0.13612 and 1.28282, which indicate the first-order approximate solution gives a reasonable prediction.

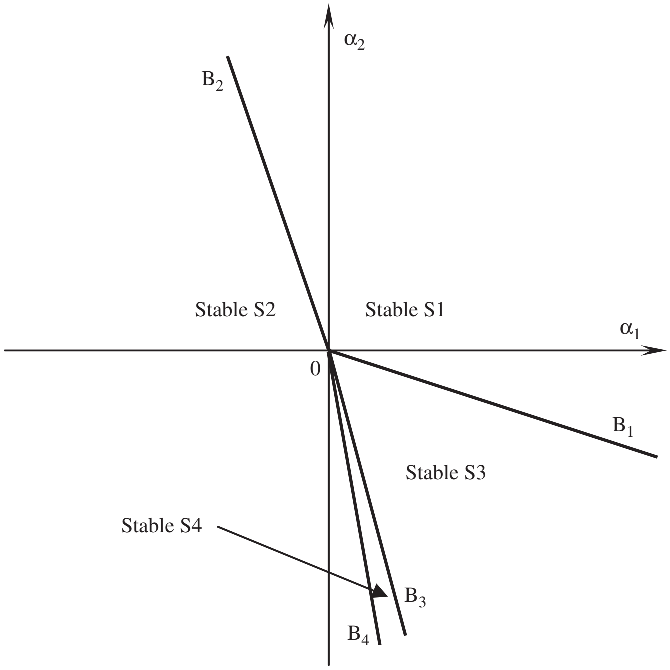

Fig. 2. Bifurcation diagram in the perturbation parameters (α_1, α_2) plane for the nonresonant co-dimension two bifurcation of Hopf–Hopf interactions.

When $(\alpha_1, \alpha_2) = (0.001, -0.0035)$, solution S3 is obtained, as shown in Fig. 3c. It is easy to find from Eq. (61) that the amplitude and frequency of solution S3 are $r_2 = 0.07969$ and $\omega_{H2} = 3.918$. Thus the first-order approximate solution of S3 may be obtained in terms of the original variables as

$$x = 0.079699\cos(0.7171t).$$

The results of numerical integration of Eq. (3) show that the amplitude and frequency of the periodic solution are 0.07719 and 0.7156, which imply the analytical predictions agree well with the numerical solutions.

A numerical solution for a quasi-periodic motion on a 2D torus (that is solution S4), as shown in Fig. 3d, is obtained by choosing the perturbation parameters as $(\alpha_1, \alpha_2) = (0.001, -0.0053)$, which is located in the region bounded by the critical lines B_3 and B_4. The two frequencies of solution S4 found by the numerical integration are 1.2848 and 0.71815. The analytical results for the frequencies are 1.28309 and 0.71783, which present a prediction close to the numerical results. It is found from Eq. (63) that the amplitudes of solution S4 are 0.05865 and 0.0494, while the numerical integration of Eq. (3) gives the amplitudes of the 2D solution as 0.0544 and 0.0415, respectively. It can be concluded that the analytical predictions of the amplitudes and frequencies are good representatives of the numerical results.

6. Summary and discussion

A controlled van der Pol–Duffing oscillator with time delay involved in the nonlinear feedback control has been studied in detail to explore a rich dynamic behaviour of the system in the vicinity of nonresonant Hopf bifurcations. The system may exhibit the initial equilibrium solution, periodic solutions with the frequencies of the first and second Hopf bifurcations, quasi-periodic solutions on 2D torus, depending on the dummy unfolding parameters and nonlinear terms. Numerical results have been given to illustrate an interaction of supercritical–supercritical Hopf bifurcations occurring in a specific system.

In the present paper, the behaviour of nonresonant Hopf bifurcations has been investigated for the corresponding autonomous system in which no external excitations are involved (that is by letting $e = 0$ in Eq. (1)). The forced response of the controlled system with time delays has received less attention in the available literature. The characterization of the forced response of the controlled system has practical

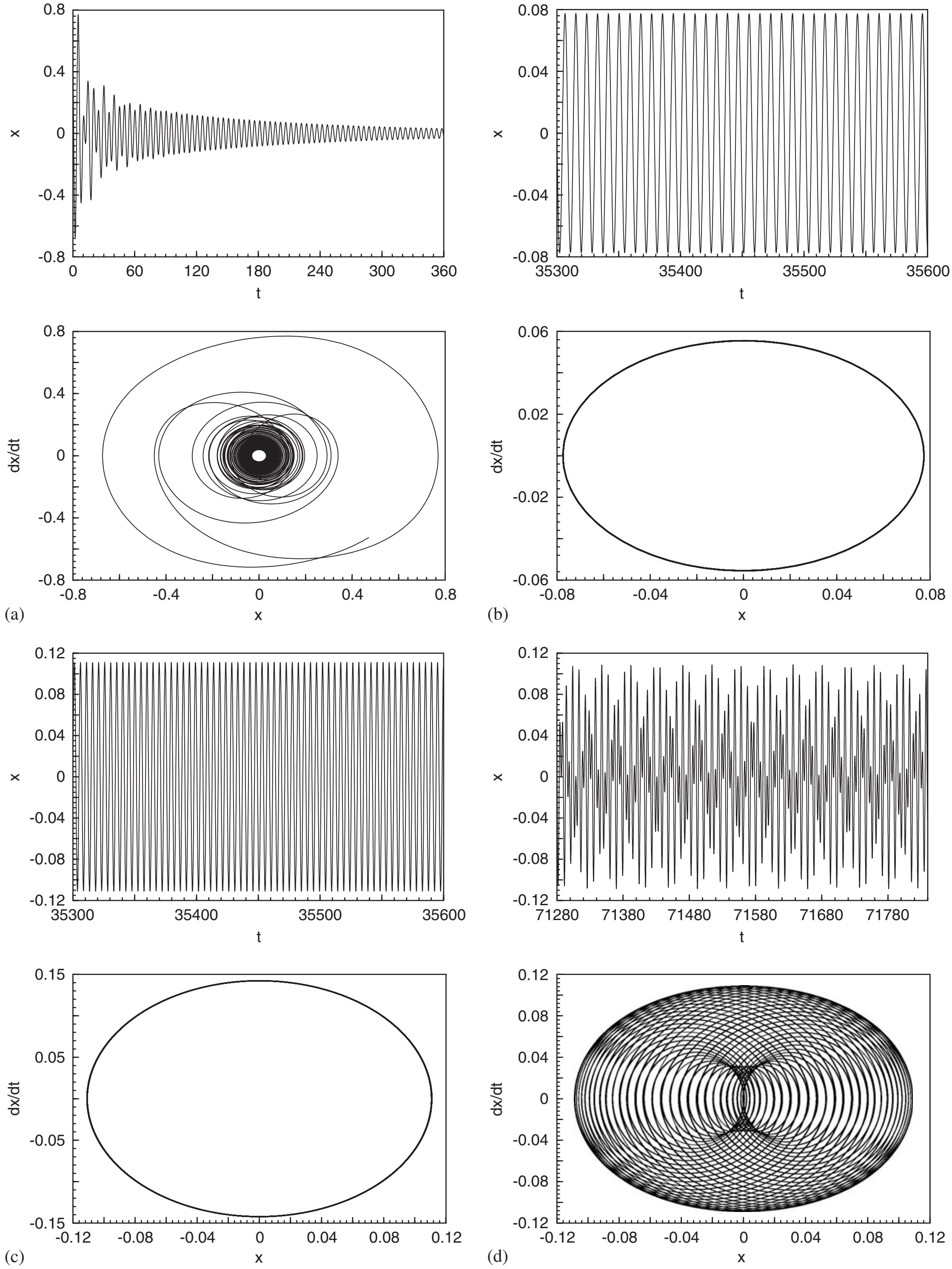

Fig. 3. Time trajectories and phase portraits of solutions of the controlled system in the neighbourhood of the nonresonant co-dimension two bifurcation of Hopf–Hopf interactions: (a) solution S1, (b) solution S2, (c) solution S3, and (d) solution S4.

significance, as many physical systems are often subjected to external driving forces. When an external excitation is presented in the controlled system involving time delay, an important technical issue that needs to be addressed is the interaction of the external excitation and the behaviour of the corresponding autonomous system that results from a nonresonant Hopf bifurcation. Such an analysis will be the subject of future research. It is conjectured that the non-autonomous system may exhibit periodic and quasi-periodic as well as chaotic motions. Some types of resonances including primary, super- and sub-harmonic resonances, additive and difference resonances will appear in the forced response of the controlled system, when the frequency of the external excitation and the frequencies of Hopf bifurcations satisfy a certain relationship.

References

[1] J.X. Xu, J. Jiang, Global bifurcation characteristics of the forced van der Pol oscillator, *Chaos, Solitons and Fractals* 7 (1996) 3–14.
[2] G.V. Belyakova, L.A. Belyakov, On bifurcations of periodic orbits in the van der Pol–Duffing equation, *International Journal of Bifurcation and Chaos* 7 (1997) 459–462.
[3] W. Szemplinska Stupnicka, J. Rudowski, The coexistence of periodic, almost-periodic and chaotic attractors in the van der Pol–Duffing oscillator, *Journal of Sound and Vibration* 199 (1997) 165–175.
[4] A. Maccari, The response of a parametrically excited van der Pol oscillator to a time delay state feedback, *Nonlinear Dynamics* 26 (2001) 105–119.
[5] A. Algaba, F. Fernandez-Sanchez, E. Freire, E. Gamero, A.J. Rodriguez-Luis, Oscillation-sliding in a modified van der Pol–Duffing electronic oscillator, *Journal of Sound and Vibration* 249 (2002) 899–907.
[6] X.B. Liu, K.M. Liew, On the stability properties of a van der Pol–Duffing oscillator that is driven by a real noise, *Journal of Sound and Vibration* 285 (2005) 27–49.
[7] G.R. Chen, J.L. Moiloa, H.O. Wang, Bifurcation control: theories, methods, and applications, *International Journal of Bifurcation and Chaos* 10 (2000) 511–548.
[8] J.C. Ji, Local bifurcation control of a forced single-degree-of-freedom nonlinear system: saddle-node bifurcation, *Nonlinear Dynamics* 25 (2001) 369–382.
[9] A.Y.T. Leung, J.C. Ji, G.R. Chen, Resonances control for a forced single-degree-of-freedom nonlinear system, *International Journal of Bifurcation and Chaos* 14 (2004) 1423–1429.
[10] F.M. Atay, van der Pol's oscillator under delayed feedback, *Journal of Sound and Vibration* 218 (1998) 333–339.
[11] J.C. Ji, A.Y.T. Leung, Resonances of a nonlinear SDOF system with two time-delays in linear feedback control, *Journal of Sound and Vibration* 253 (2002) 985–1000.
[12] J.C. Ji, A.Y.T. Leung, Bifurcation control of a parametrically excited Duffing system, *Nonlinear Dynamics* 27 (2002) 411–417.
[13] A. Maccari, Vibration control for the primary resonance of the van der Pol oscillator by a time delay state feedback, *International Journal of Non-Linear Mechanics* 38 (2003) 123–131.
[14] A. Maccari, Vibration control for parametrically excited Lienard systems, *International Journal of Non-Linear Mechanics* 41 (2006) 146–155.
[15] J.C. Ji, C.H. Hansen, Stability and dynamics of a controlled van der Pol–Duffing oscillator, *Chaos, Solitons and Fractals* 28 (2006) 555–570.
[16] S.A. Campbell, J. Belair, T. Ohira, J. Milton, Limit cycles, tori and complex dynamics in a second-order differential equation with delayed negative feedback, *Journal of Dynamics and Differential Equations* 7 (1995) 213–236.
[17] J.C. Ji, Stability and bifurcation in an electromechanical system with time delays, *Mechanics Research Communications* 30 (2003) 217–225.
[18] J.C. Ji, Stability and Hopf bifurcation of a magnetic bearing system with time delays, *Journal of Sound and Vibration* 259 (2003) 845–856.
[19] Z.H. Wang, H.Y. Hu, H.L. Wang, Robust stabilization to non-linear delayed systems via delayed state feedback: the averaging method, *Journal of Sound and Vibration* 279 (2005) 937–953.
[20] J.J. Wei, W.H. Jiang, Stability and bifurcation analysis in van der Pol's oscillator with delayed feedback, *Journal of Sound and Vibration* 283 (2005) 801–819.
[21] B.D. Hassard, N.D. Kazarinoff, Y.H. Wan, *Theory and Applications of Hopf Bifurcations*, Cambridge University Press, Cambridge, 1981.
[22] S.A. Campbell, J. Belair, Resonant co-dimension two bifurcation in the harmonic oscillator with delayed forcing, *Canadian Applied Mathematics Quarterly* 7 (1999) 218–238.
[23] J. Hale, *Theory of Functional Differential Equations*, Springer, New York, 1977.
[24] J.K. Hale, S.M. Verduyn Lunel, *Introduction to Functional Differential Equations*, Springer, New York, 1983.
[25] A. Halanay, *Differential Equations, Stability, Oscillations, Time Lags*, Academic Press, New York, 1966.
[26] A.H. Nayfeh, D.T. Mook, *Nonlinear Oscillations*, Wiley, New York, 1979.
[27] P. Yu, A.Y.T. Leung, A perturbation method for computing the simplest normal forms of dynamical systems, *Journal of Sound and Vibration* 261 (2003) 123–151.
[28] J. Guckenheimer, P. Holmes, *Nonlinear Oscillations, Dynamical Systems, and Bifurcations of Vector Fields*, Springer, New York, 1983.